

Interaction of Silver Nanoparticles with Polymers and Surfactants

M.Sc. Thesis

By

PUSHPENDER YADAV



DISCIPLINE OF CHEMISTRY
INDIAN INSTITUTE OF TECHNOLOGY INDORE

JUNE 2018

Interaction of Silver Nanoparticles with Polymers and Surfactants

A THESIS

*Submitted in partial fulfillment of the
requirements for the award of the degree
of*
Master of Science

by
PUSHPENDER YADAV

1603131014



DISCIPLINE OF CHEMISTRY
INDIAN INSTITUTE OF TECHNOLOGY INDORE

JUNE 2018



INDIAN INSTITUTE OF TECHNOLOGY INDORE

CANDIDATE'S DECLARATION

I hereby certify that the work which is being presented in the thesis entitled **Interaction of Silver Nanoparticles with Polymers and Surfactants** in the partial fulfillment of the requirements for the award of the degree of **MASTER OF SCIENCE** and submitted in the **DISCIPLINE OF CHEMISTRY, Indian Institute of Technology Indore**, is an authentic record of my own work carried out during the time period from July 2017 to June 2018 under the supervision of **Dr. TUSHAR KANTI MUKHERJEE**, Associate Professor, Discipline of Chemistry, IIT Indore.

The matter presented in this thesis has not been submitted by me for the award of any other degree of this or any other institute.

**Signature of the student with date
PUSHPENDER YADAV**

This is to certify that the above statement made by the candidate is correct to the best of my/our knowledge.

Signature of the Supervisor

(Dr. TUSHAR KANTI MUKHERJEE)

PUSHPENDER YADAV has successfully given his M.Sc. Oral Examination held on 6 July 2018

Signature of Supervisor of M.Sc. thesis
Date:

Convener, DPGC
Date:

Signature of PSPC Member
Date:

Signature of PSPC Member
Date:

ACKNOWLEDGEMENT

I express my heartfelt gratitude to my thesis supervisor Dr. Tushar Kanti Mukherjee for his support and constructive guidance throughout my work. His confidence, enthusiasm, and dedication have been always inspirational. His deep insights and suggestions helped me a lot at various stages of my research project. His patience, understanding, and motivation have been always helpful for the completion of this journey.

I am thankful to my PSPC members, Dr. Anjan Chakraborty and Dr. Satyajit Chatterjee for their guidance and valuable suggestions during my work.

I wish to express my gratitude to Prof. Pradeep Mathur, Director, IIT Indore for his continuous support in every aspect.

I would also like to thank Dr. Satya S. Bulusu, Dr. Tridib Kumar Sarma, Dr. Apurba Kumar Das, Dr. Sanjay Kumar Singh, Prof. Suman Mukhopadhyay, Dr. Biswarup Pathak, Dr. Shaikh M. Mobin, Prof. Rajneesh Misra, Dr. Sampak Samanta, Dr. Chelvam Venkatesh, and Dr. Amrendra Kumar Singh for their guidance and help during various activities in the department.

I extend my deep thanks to my group members Dr. Arpan Bhattacharya , Dr. Roopali Prajapati , Ms. Jamuna Vaishnav, Mr. Ashish Raikwar, Mrs. Shallu Tanwar for their generous help and co-operation. My classmates will always be remembered for understanding and supporting me in all the phases throughout my M.Sc.

I would also like to thank Ms. Sarita Batra, Mr. Kinny Pandey, Mr. Ghanshyam Bhavsar, Mr. Ravinder Kumar, Mr. Manish Kushwaha, Ms. Vinita Kothari, and Mr. Rameshwar Dauhare for their technical support. I would also like to thank Ms. Anjali Bandiwadkar, Mr. Rajesh Kumar, Mr. Lala Ram Ahirwar and other library staffs for their constant help, whenever required. Further, I would like to acknowledge SIC, IIT Indore for instrumentation facilities.

Most importantly, it would have been impossible for me to reach here without the support, care, and love of my family. I express my respect, love, and gratitude to my beloved maternal grandparents Mr. Ram Kumar and Mrs. Kamla Devi, my parents Mr. Surender Kumar and Mrs. Madhubala, my elder brother Mr. Lokendra Rao and my sister in law Mrs. Ekta Yadav for their unconditional love and support.

I thank each and every single person who, knowingly or unknowingly, helped me during this time.

PUSHPENDER YADAV

Dedicated to
My Family....

ABSTRACT

In the present work, we have seen the interaction of small sized citrate capped Ag NPs with polymers and the surfactants. The capping agent used in Ag NPs to stabilize them is negatively charged and its interaction with the positively charged polymer and positively charged surfactant shows good and stable aggregation of Ag NPs. Cationic PDADMAC shows electrostatic interaction with Ag NPs which is confirmed by comparing the results with the interaction of Ag NPs with neutral polymer PVP, anionic surfactant SDS and neutral surfactant TX-100 using UV-Vis spectrometer. The hydrodynamic size of aggregated Ag NPs were also calculated using dynamic light scattering (DLS) and these aggregation are studied using PL microscopy and morphology of polymer in absence and presence of Ag NPs using FE-SEM. On the other hand we have used cationic surfactant instead of polymer to study the aggregation of Ag NPs and further extent the interaction of these surfactant induced aggregation with neutral polymer PVP and perform UV-Vis spectroscopy, PL microscopy to visualize the type of interaction (i.e. hydrophobic or electrostatic) in between PVP and the surfactant using Ag NPs aggregation as PL marker.

TABLE OF CONTENTS

LIST OF FIGURES	xi
LIST OF SCHEMES	xiii
LIST OF TABLES	xiv
NOMENCLATURE	xv
ACRONYMS	xvi
Chapter 1: Introduction	1-8
1.1. Metal Nanoparticles (NPs)	1
1.2. NPs and Polymer interaction	2
1.3. Surfactant Assemblies	5
1.4. Aggregation of Ag NPs and its interaction with polymers	6
Chapter 2: Experimental Section	9-12
2.1. Chemicals	9
2.2. Synthesis of citrate capped Ag NPs	9
2.3. Sample Preparation	10
2.4. Instrumentation	11
2.4.1 UV-Vis Spectrophotometer	11
2.4.2. Field-Emission Scanning Electron Microscope (FE-SEM)	11
2.4.3. Dynamic Light Scattering (DLS) and Zeta Potential	11
2.4.4. Epifluorescence Microscopy	11
Chapter 3: Results and Discussion	13-22
3.1 Characterization of Ag NPs	13
3.2. Interaction between Ag NPs and cationic Polymer PDADMAC	13
3.3. Surfactant induced aggregation of Ag NPs and interaction with PVP	19
Chapter 4: Conclusion and Scope for the future work	23
REFERENCES	24

LIST OF FIGURES

Figure 1.2	Structure of Poly (diallyldimethylammonium) Chloride.	2
Figure 1.3	The chemical structures of CTAB, SDS, and TX-100.	5
Figure 1.4	Two possible “Necklace and Bead” models.	7
Figure 3.1	(A) The size distribution histogram of Ag NPs from DLS measurement.	13
Figure 3.1	(B) Absorption spectra of Ag NPs.	13
Figure 3.2	(A) Change in absorption spectra of Ag NPs with gradual addition of wt % of PDADMAC.	14
Figure 3.2	(B) Change in absorption peak at ($\lambda=575$ nm and 391nm) at different wt % [PDADMAC].	14
Figure 3.2	(C) Change in the absorbance spectra of Ag NPs in the presence of SDS, TX-100, PVP.	14
Figure 3.2	(D) The size distribution histogram of Ag NPs with 2.5 wt % PDADMAC from DLS measurement.	16
Figure 3.2	(E)(a) FE- SEM image of PDADMAC.	16
	(b) FE-SEM image of Ag NPs –polymer mixture.	16
Figure 3.2	(F) PL image of Ag NPs; (G) PL Intensity profile of Ag NPs.	17
Figure 3.2	(H) PI image; (I) PL Intensity profile of Ag NPs in the presence of 2.5 wt % PDADMAC.	18
Figure 3.3	(A) Change in absorption spectra of Ag NPs upon addition of different molar concentration of CTAB.	19
Figure 3.3	(B) PL image ;(C) PL Intensity profile of Ag NPs in the presence of 0.2 mM CTAB.	20

Figure 3.3 (D) Change in the absorption spectra of Ag NPs in 21
the presence of PVP.

Figure 3.3 (E) PL Image; (F) PL Intensity profile of CTAB- 22
Induced Ag NPs aggregation in 0.5 wt % PVP.

LIST OF SCHEMES

Scheme 1.	Electronic energy levels of metal NC, NP, and bulk metal.	1
Scheme 2.	Possible mechanism for the anti aggregation of citrate capped Ag NPs in phosphate buffer.	5
Scheme 3.	Representation of the surfactant assemblies in solution.	6
Scheme 4.	Proposed Model for CTAB bilayer-Induced Aggregation of Ag NPs.	7
Scheme 5.	Schematic representation of our home-built epifluorescence microscope.	12

LIST OF TABLES

Table 1.	Required amount of reagents for the synthesis of small sized Ag NPs.	10
-----------------	--	----

NOMENCLATURE

a.u.	Arbitrary unit
°	Degree
λ_{ex}	Excitation Wavelength
μm	micrometer
μM	micromolar
mM	millimolar
nm	nanometer
R_G	radius of gyration
σ_{rep}	electrostatic repulsion
Q	charge
nM	nanomolar
mm	millimeter

ACRONYMS

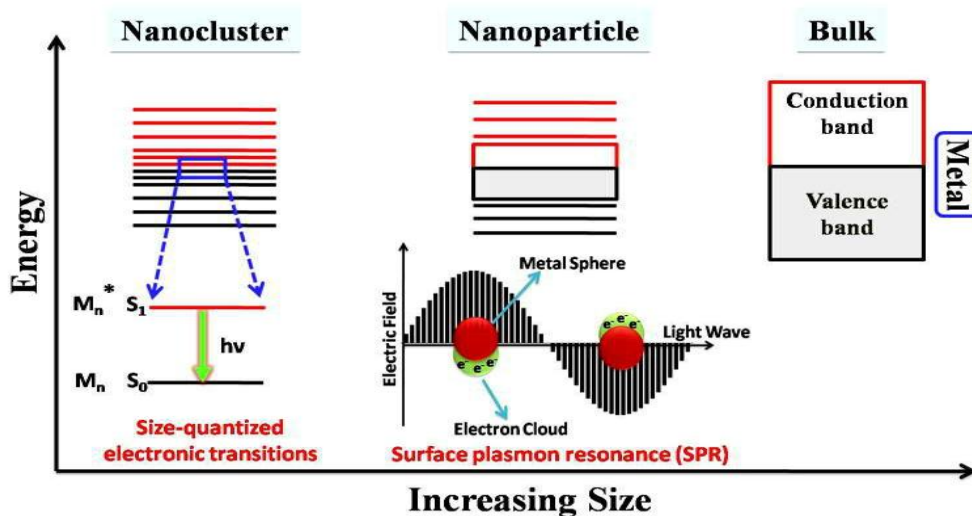
AFM	Atomic force microscopy
Ag NC	Silver nanocluster
Ag NP	Silver nanoparticles
CMC	Critical micelles concentration
CTAB	Cetyltrimethylammonium bromide
DLS	Dynamic light scattering
FL	Fluorescence
FE-SEM	Field-emission scanning electron microscope
LSPR	Localized surface Plasmon resonance
O.D.	Optical density
PDADMAC	Poly (diallyldimethylammonium) chloride
PL	Photoluminescence
QDs	Quantum dots
SDS	Sodium dodecyl sulphate
SERS	Surface enhanced Raman scattering
TX-100	Tritn X-100
UV	Ultraviolet
Vis	Visible

CHAPTER 1

1. INTRODUCTION

1.1. Metal Nanoparticles

In recent years, metallic nanoparticles (NPs) have attracted considerable interest due to their interesting physicochemical properties, small size and surface plasmon behavior. The electronic and optical properties of metal NPs greatly depends on their size, particularly in the nanometer range (Scheme 1.1) [1-3]. Bulk metals are electrically conducting and good optical reflectors due to the freely moving delocalized electrons in the conduction band. Metal NPs (2-100 nm) display intense colors as a result of the localized surface plasmon resonance (LSPR). The application of Ag NPs is fundamentally based on their intrinsic LSPR effect which occurs due to the collective coherent oscillations of conduction electrons near the metal/dielectric interfaces when the size of the NPs is much smaller than the wavelength of the incident light [4]. These oscillations are very sensitive to any change of this boundary, such as the adsorption of molecules to the conducting surface.



Scheme 1. Electronic energy levels of metal nanocluster (NC), NP, and bulk metal.

Spherical NPs are considered to be the best for practical applications in either colloidal form, or immobilized state [5, 6]. Among all metallic NPs, Ag NPs have been used in different fields including optoelectronics, biosensors, antimicrobials catalysis, surface enhanced Raman scattering (SERS), near-field scanning probe microscopy, luminescence enhancement and quenching at the metal surface, etc [7-13]. The shape and size of the Ag NP directly influence its characteristic LSPR band. The LSPR maximum (λ_{LSPR}) of spherical Ag NP ranges from 390-500 nm depending on the size of the Ag NP [9, 10]. With the increase in the size of NPs, the λ_{LSPR} shifts to the longer wavelength. Further, an additional LSPR effect can be observed when the spacing between particles is small enough to delocalize surface electrons causing plasmon coupling which shifts LSPR band to higher wavelength and indicates aggregation [14-16]. In the present work, small sized citrate-capped Ag NPs exhibiting λ_{LSPR} at 390 - 400 nm have been synthesized by the well-known Lee and Meisels method with slight modifications [17].

1.2. NPs and Polymer Interaction

The practical significance of cationic water soluble polyelectrolyte's has increased rapidly since many years. Its applications are developed by greater extent due to increased use in dewatering agents and emulsifiers in processes of water purification, papermaking, mining and petrol industry as well as the application as additives thus determining the final properties of products mainly of the cosmetics industry [18].

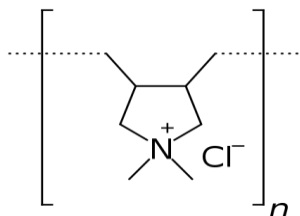


Figure 1.2 Structure of Poly(diallyldimethylammonium chloride)

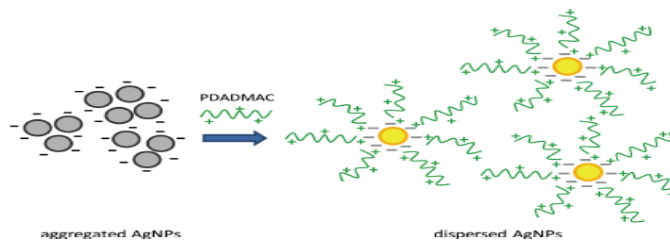
Poly(diallyldimethylammonium chloride) (PDADMAC) is a typical representative of a water-soluble polyelectrolyte having hydrophilic positively charged quaternary ammonium groups. PDADMAC is used for the preparation of magnetic core– shell particles [19, 20], capsules [21] for the preparation of multilayer films on solid substrate such as: silicon wafers, quartz, gold or on porous and soft microgels [22]. Furthermore, PDADMAC is often used as a model for studies in different areas of polyelectrolyte research, e.g., in the interaction with oppositely charged soluble polymers and with colloids.

Aqueous solutions having polyelectrolytes and charged particles have received greater attention because of their applications in the field of water treatment to promote the rate of coagulation, in food technology and in powder processing to facilitate powder handling and transfer processes [23, 24]. The separation of solid particles from a dispersion fluid is very difficult, with implications for water treatment. This separation is often obtained through the addition of dissolved polymers that adsorb on the surfaces of the particles, overcome the repulsions between them and, by disturbing suspension, collect all the particles having macroscopic aggregates. The growth of these flocs is much faster than the regular aggregation processes which depend on random collisions between particles. Due to the strong adsorbing capability of polyelectrolytes on surface having opposite charge can be used as a polymer glue to hold the particles together [25]. The stability of colloidal dispersions can be altered through the addition of adsorbing macromolecules and results in a stepwise aggregation process. The interaction between the surface of a colloid/NPs and polymers can be repulsive or attractive. When monomers of the polymers and the surfaces of the NPs attract each other, an adsorbed layer is formed which modifies the effective interaction between the particles. The adsorption of NPs on the surfaces of oppositely charged polyelectrolyte is complicated because of the long range nature of electrostatic interaction. Several theoretical efforts have been produced in

the last few years [26]. Two main predictions were made , (i) First, a small sphere of central charge Q homogeneously distributed ,can adsorb and collapse a polyelectrolyte of charge $-Q$, greater in absolute value than the initial charge Q . This charge reversal of the colloid is due to the connection between charges and the correlation in the adsorbed state. The reversal in charge increases with salt concentration and have maximum when the polyelectrolyte is long enough to just saturate the colloid without any tail remains in the ‘free’ solution. (ii) Second, beyond a threshold chain length, one or two tails remains in the ‘free’ solution which means the solid surfaces are no more saturated with macromolecules and a possibility of cross-linking between two necklaces [27]. Spalla *et al* (1993) [28] have shown the stability of dispersion of colloid is formed by electrostatic repulsions between particles, and destabilization may occur from polymer-induced attractions. They started with a stable dispersion of particles, where the range of repulsions is set by the ionic strength. Macromolecules addition causes the formation of finite aggregates; particles to polymer ratio tells about the structure of these aggregated. When the range σ_{rep} of electrostatic repulsions is longer than the radius of gyration R_G (the mass weighted average distance from the core of a molecule to each mass element in the molecule) of the macromolecules, bridges cannot be established and the particles remain independent from each other. When σ_{rep} is lower than R_G , bridging is possible and multiplet structures are possibly formed. Finally, when σ_{rep} is below than critical distance, which is twice the particle diameter, the multiplets may bind to each other and they form macroscopic flocs.

Trisaranakul *et al* (2009) [29] have recently shown that by forming aggregates of Ag NPs using buffer solution and adding PDADMAC into the aggregated solution, the polymer can adsorb onto the particle surface *via* electrostatic interaction between its positively charge polymer and negatively charged citrate. Ag NPs are then anti- aggregated by the cationic repulsive and steric forces of polymer (Scheme 2). By measuring

the change in SPR of NPs, they calculate the quantity of PDADMAC present in water.



Scheme 2. Possible mechanism for the anti aggregation of citrate capped Ag NPs in phosphate buffer.

In the present work, we have used freshly prepared small sized Ag NPs in Mill-Q water and have shown its interaction with positively charged PDADMAC and proposed that electrostatic attraction is the main force between NPs and polymer which results in the aggregation by comparing UV – Vis spectroscopic result of Ag NPs with neutral polymer, neutral and positively charged surfactant.

1.3. Surfactant Assemblies

The surfactant is an amphiphilic molecule containing a non-polar hydrocarbon tail and a polar head group. The tail of a surfactant can be linear, branched or aromatic and the polar head group can be neutral or ionic depending upon the charge it carries. The chemical structures of the cationic surfactant cetyltrimethylammonium bromide (CTAB), anionic surfactant sodium dodecyl sulfate (SDS), and neutral surfactant tritons X-100 (TX-100) are shown in Figure 1.3.

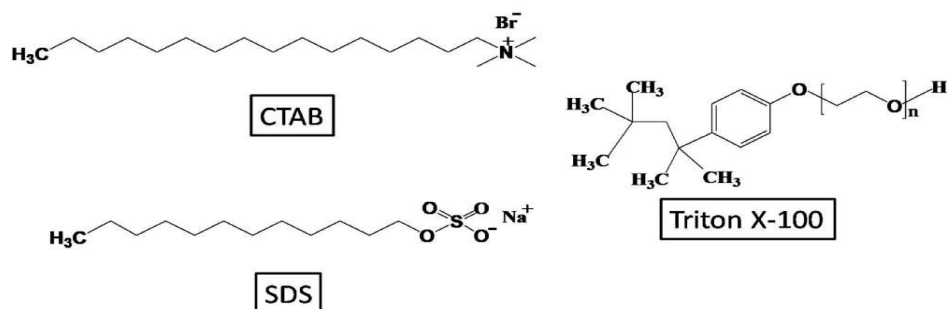
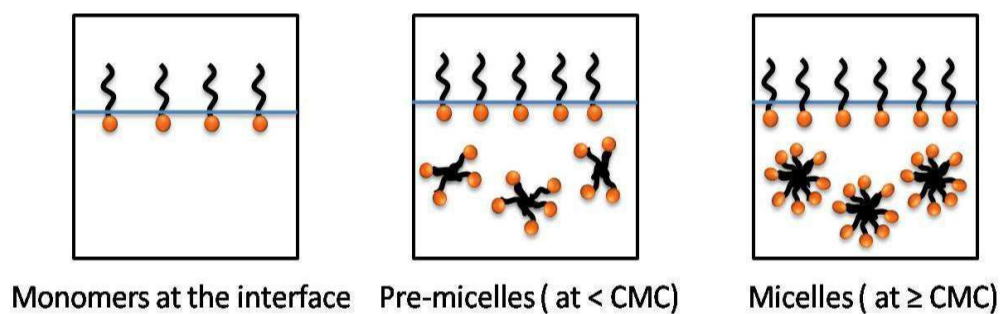


Figure 1.3 The chemical structures of CTAB, SDS and TX-100.

At very low concentration of surfactant, the polar group remains in the aqueous phase and hydrophilic tails points towards the air and forms a monolayer at water – air interface. Further addition of surfactant results in the formation of pre-micelles aggregates in the solution followed by formation of spherical aggregated at or beyond the critical micelle concentration (CMC). (Scheme 3)

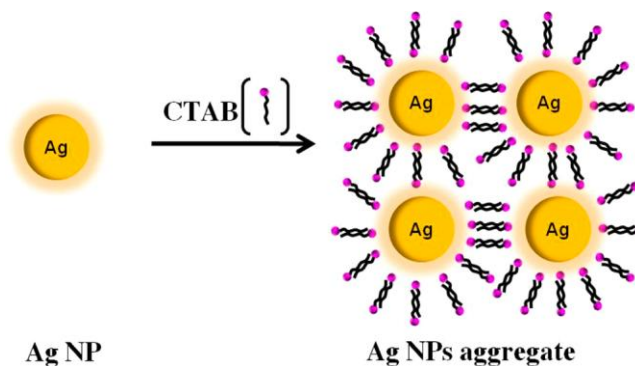


Scheme 3. Representation of the surfactant assemblies in solution.

The CMC of above-mentioned surfactants CTAB, SDS, and TX-100 is 1, 8, and 0.22 mM, respectively.

1.4. Aggregation of Ag NPs and its Interaction with Polymers

In earlier studies, it is shown that changes in the LSPR band of Ag NPs in the presence of CTAB indicate the formation of surfactant-induced aggregates of Ag NPs. The red shift observed in UV-Vis spectra with significant spectral broadening in the LSPR of Ag NPs indicates the coupling of the surface plasmon of the closely spaced Ag NPs in the aggregates. Moreover, in the presence of negatively charged SDS and neutral TX-100 surfactant these spectral changes are absent which indicated that the aggregates are formed due to the specific electrostatic interactions between the negatively charged citrate molecules on the surface of Ag NPs and positively charged CTAB head groups [30].(scheme 4)



Scheme 4. Model for CTAB bilayer-induced aggregation of Ag NPs.

These surfactant induced aggregates binds with the polymer in “necklace and bead” like morphology below their normal CMC and are attached with the polymer chain with some specific interaction (hydrophobic, dipolar or electrostatic). Earlier, two models for “necklace and bead”-like structures have been proposed for polymer–surfactant complexes: one having the surfactant aggregates attached on the hydrophobic sites of the polymer chain, where surfactant head groups are exposed to surrounding water, and the other with the polymer chain wrapped around the surfactant aggregates, where the surfactant head groups are associated with the polymeric chain (Figure 1.4).

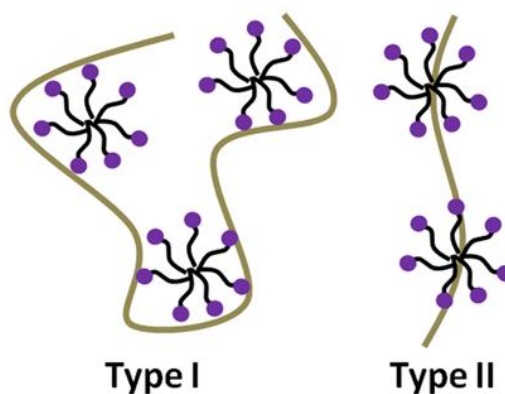


Figure 1.4 Two possible “Necklace and Bead” models.

Earlier our group have shown the initial complexes formed between negatively charged surfactant SDS with neutral poly(vinylpyrrolidone) (PVP) polymer through photoluminescence (PL) microscopy and atomic

force microscopy (AFM) using silicon quantum dot (Si QD) as an external PL marker. It was observed that, for the PVP–SDS system, SDS molecules bind at the hydrophobic sites on the random-coiled PVP chain through their hydrocarbon tails.

In this present work, we have taken CTAB as surfactant which produces Ag NPs aggregates (Scheme 4) and made an attempt to see the interaction between these aggregates and PVP, by using Ag NPs as external PL marker with the help of PL microscopy.

CHAPTER 2

2. EXPERIMENTAL SECTION

2.1. Chemicals

Silver nitrate (AgNO_3 , $\geq 99\%$), cetyltrimethylammonium bromide (CTAB, $\geq 98\%$), triton X-100 (TX-100, AR grade), sodium dodecyl sulfate (SDS, 98.5%), methanol, neutral polymer PVP (MW = 40 000), cationic poly(diallyldimethylammoniumchloride) (PDADMAC, MW= 100000-200000) were purchased from Sigma-Aldrich. Tri-sodium citrate dihydrate (TSC), sulphuric acid (H_2SO_4 , 98 %), were purchased from Merck (Germany). Sodium borohydride (NaBH_4) was purchased from SRL. Milli-Q water was obtained from a Millipore water purifier system (Milli-Q integral).

2.2. Synthesis of Citrate Capped Ag NPs

Citrate capped Ag NPs were synthesized using sodium borohydride (NaBH_4) as an essential reductant and trisodium citrate (TSC) as both secondary reductant and stabilizing agent. This synthesis was carried at two different temperature i.e. 60 °C and 90 °C mediated mainly by NaBH_4 and TSC. A simple methodology is as per the following: the required volumes of aqueous solutions containing NaBH_4 and TSC were mixed and heated to 60 °C for 30 minutes with vigorous stirring to ensure a homogenous solution in a dark surrounding. At the end of 30 minutes, the required volume of AgNO_3 solution was added drop-wise to the mixture and in this way, the temperature was additionally raised to 90 °C. As the temperature came to 90 °C, the pH of the mixture was changed to 10.5 using 0.1 M NaOH while heating was proceeded for 20 minutes, until the colour changed. The NPs suspension was permitted to cool at room temperature. With a specific end goal to evacuate the unreacted reductants, Ag NPs suspensions were centrifuged (12 000 rpm, 15 minutes) and washed thrice, trailed by redispersion in DI water and were finally put

away at 4 °C for future utilize. We have synthesized small sized Ag NPs of size 10-20 nm having λ_{LSPR} 391 – 400 nm.

Particle size(nm)	AgNO ₃ (mol dm ⁻³)	NaBH ₄ (mol dm ⁻³)	TSC (mol dm ⁻³)	Volume of reactants (ml)
15 nm	1.00×10^{-03}	1.00×10^{-03}	1.06×10^{-03}	x=48, y=2

x- total volume of NaBH₄ and TSC ; y-volume of AgNO₃ added drop wise to x

Table.1 Required amount of reagents for the synthesis of small sized Ag NPs.

2.3. Sample Preparation

The Synthesized Ag NPs (16.6 nM) were further diluted as per experimental requirement using Milli-Q water. The aqueous stock solutions of 0.1 M CTAB , 0.1 M SDS and 0.2 M TX-100 were prepared by dissolving the required amount of chemicals in Milli-Q water and for further experiments the aqueous stock solutions of CTAB , SDS and TX - 100 were diluted using Milli-Q water. PDADMAC was used directly from the stock solution (20 wt %) according to the required weight percentage. 20 wt % of PVP was also prepared as stock solution and used directly from the solution according to the required weight percentage . For PL microscopy experiment, the samples were spin coated on a clean cover slide with a spin coater (Apex Instruments, Spin NXG-P1) and for the SEM, samples were drop casted in vacuum overnight. Cover slides cleaning was done by using chromic acid, followed by 2% Hellmanex III (Sigma-Aldrich). Each of the cleaning steps was followed by repeated washing with Milli-Q water. Finally, the washed slides were rinsed with methanol and dried in vacuum oven. The samples were spin cast on cover slides at 1000 rpm for 3 min.

2.4. Instrumentation

2.4.1 UV-Vis Spectrophotometer

Absorption spectra were recorded in a quartz cuvette (10 × 10 mm) using a Varian UV-Vis spectrophotometer (Carry 100 Bio) and were corrected using solvent absorption as the baseline.

2.4.2. Field-Emission Scanning Electron Microscope (FE-SEM)

The morphologies of Ag NPs with PDADMAC were estimated using FE-SEM technique. The SEM images were recorded by using FE-SEM, Supra 55 Zeiss. The samples were drop casted overnight on slide followed by the gold coating.

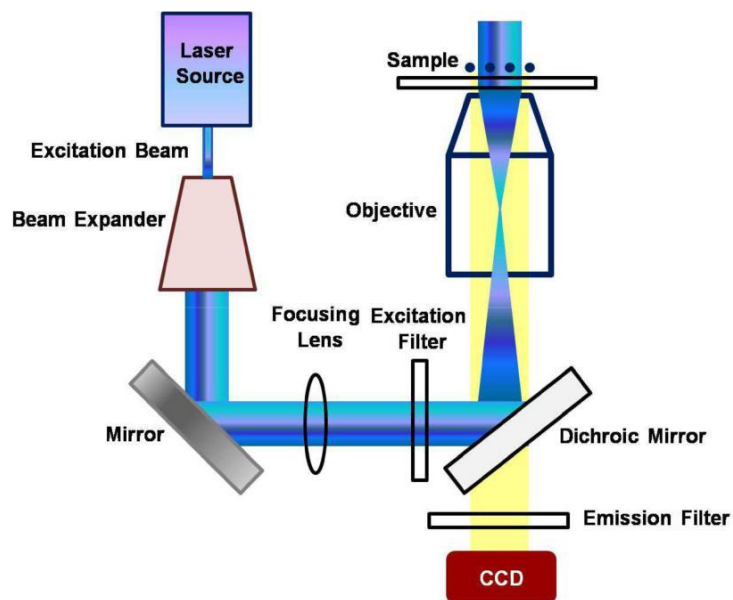
2.4.3. Dynamic Light Scattering (DLS) and Zeta Potential

DLS was used to estimate the hydrodynamic diameter of Ag NP with or without adding PDADMAC. The DLS and zeta potential measurements for Ag NPs were performed on the NanoPlus zeta/particle size analyzer (NanoPlus-3 model). All the samples for DLS and zeta potential measurements were prepared in Milli-Q water and were filtered through 0.22 µm syringe filter (Whatman) prior to measurements.

2.4.4. Epifluorescence Microscopy

Microscopy experiments were performed on a home-built epifluorescence microscopy setup (Scheme 5). An air-cooled argon ion laser (Melles Griot, model 400-A03) with excitation wavelength at 488 nm was used to excite the sample placed on an inverted microscope (Nikon, model Eclipse Ti-U). The laser beam was expanded and subsequently focused on the back-focal plane of an oil immersion objective (100× 1.49 NA Nikon) to illuminate 60 × 60 µm² area of the sample. The PL from the sample was collected through a B2A filter cube (Nikon) with a 505 nm dichroic mirror and a 520 nm long-pass filter and finally imaged with a back-illuminated EMCCD camera (Andor, model

iXon X3 897). The exposure time was 200 ms. The images were analyzed with ImageJ (Version 1.46r) NIH. All PL measurements were performed at room temperature. For microscopy experiments, the samples were spin casted with a spin-coater (Apex Instruments, Spin NXG-P1) on a clean cover slide.



Scheme 5. Schematic representation of our home-built epifluorescence microscope.

CHAPTER 3

3. RESULTS AND DISCUSSION

3.1 Characterization of Ag NPs

The synthesized citrate capped Ag NPs were characterized using UV-Vis spectra and DLS. To estimate the mean hydrodynamic diameter of synthesized Ag NPs, we performed DLS measurement. Figure 3.1 (A) shows the size distribution histogram from DLS measurements. The diameter varies from 10-30 nm with a mean diameter of 24 ± 14 nm. The absorption spectrum of Ag NPs is characterized by a strong LSPR band centered at 391 nm (Figure 3.1 B). Here it is important to mention that the position of the LSPR peak is in accordance with the estimated mean size of synthesized Ag NPs [31].

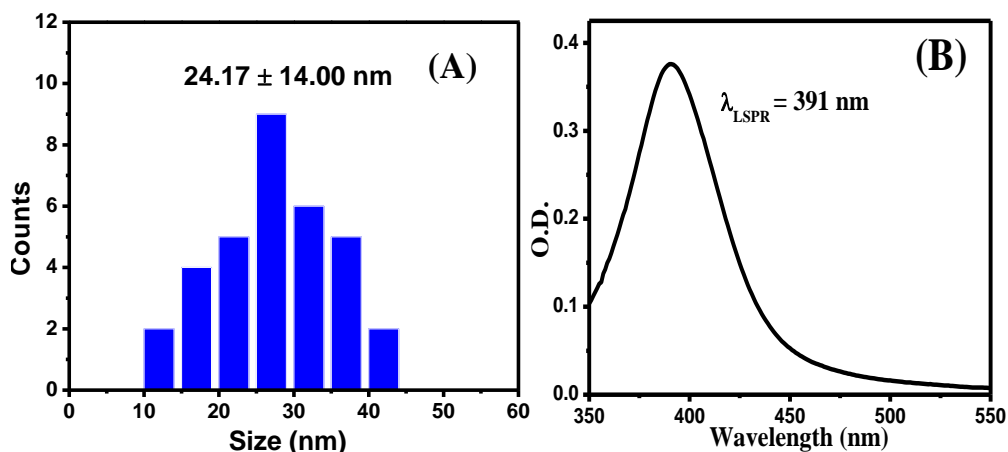


Figure 3.1 (A) The size distribution histogram of Ag NPs from DLS measurement. **(B)** Absorption spectra of Ag NPs.

3.2. Interaction between Ag NPs and Cationic Polymer PDADMAC

The absorption spectra of Ag NPs show LSPR at 391 nm in Milli-Q water. Significant spectral changes have been observed upon addition of different weight percentage (wt %) of PDAMDAC (Figure 3.2 A). At low wt % of polymer shows decrease in the absorption of Ag NPs with noticeable red shift in the peak position from 391 nm to 397 nm. However, with further

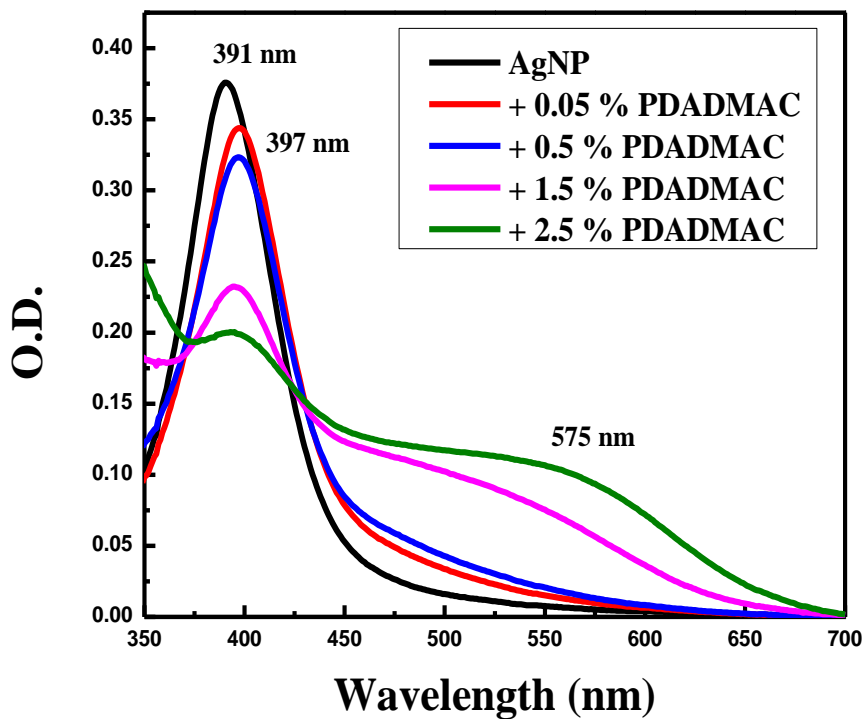


Figure 3.2 A Change in absorption spectra of Ag NPs with gradual addition of wt % of PDADMAC.

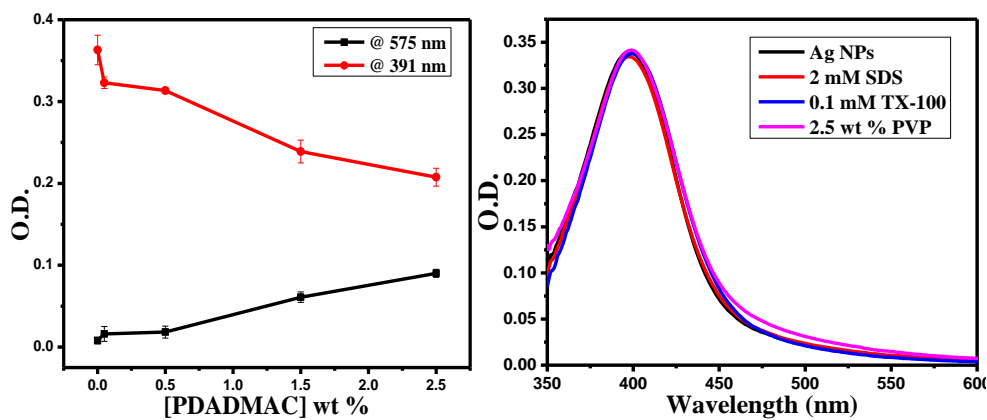


Figure 3.2 (B) Change in absorption peak at ($\lambda=575$ nm and 391 nm) at different wt % [PDADMAC]. **(C)** Change in the absorbance spectra of Ag NPs in the presence of SDS, TX-100 and PVP.

increase in concentrations of PDADMAC (1.5 wt %), the absorbance peak of Ag NPs decreases with gradual peak shift to a longer wavelength. At 2.5 wt % PDADMAC, the absorbance peak of Ag NPs progressively decreases and a broad peak centered at 575 nm appeared. The noticeable amount of red shifts observed with significant spectral broadening in the LSPR of Ag NPs can be attributed to the coupling of the surface plasmon of the closely spaced Ag NPs in the aggregates. The observed peak shifts are believed to be the result of particle aggregation as polymer induces depletion attractions. Note that depletion attraction becomes stronger with increasing polymer concentrations [32, 33]. Figure 3.2 (B) shows the change in the absorption peak of Ag NPs and the Ag NPs aggregation peak at different concentration of [PDADMAC].

To know the nature of interaction between Ag NPs and cationic PDADMAC, we have also studied the effect of neutral polymer PVP, anionic and neutral surfactant with the negatively charged Ag NPs (Figure 3.2 C). The absence of any such spectral changes in the presence of negatively charged SDS and neutral TX-100 surfactant and neutral polymer PVP indicates that the aggregates are formed due to the specific electrostatic interactions between the negatively charged citrate molecules on the surface of Ag NPs and positively charged sites on the polymer PDADMAC.

To get further details of these polymer-induced aggregations of Ag NPs, we performed DLS experiment. Figure 3.2 (D) shows the size-distribution histogram of Ag NPs in the presence of 2.5 wt % PDADMAC from DLS measurements. The sizes of Ag NPs vary from 300 to 1100 nm with a mean hydrodynamic diameter of 774.9 ± 470 nm. This increase in mean hydrodynamic diameter from 24 ± 14 nm to 774.9 ± 470 nm of Ag NPs in the presence of 2.5 wt % PDADMAC clearly shows that these Ag NPs undergo polymer-induced aggregation. To know how these Ag NPs aggregations are changing the morphology of PDADMAC while attaching

by electrostatic interaction, we performed FE-SEM. Figure 3.2 E (a) shows the image of 2.5 wt % PDADMAC having average size of 128 μm . Figure 3.2 E (b) shows FE-SEM image of polymer with Ag NPs .The addition of Ag NPs breaks the chain into smaller length (42 μm) and gets attached to it and shows aggregation as discussed in introduction.

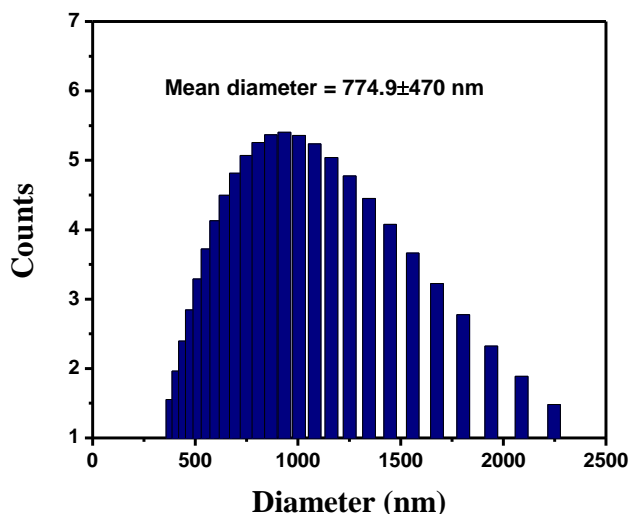


Figure 3.2 D The size distribution histogram of Ag NPs with 2.5 wt % PDADMAC from DLS measurement.

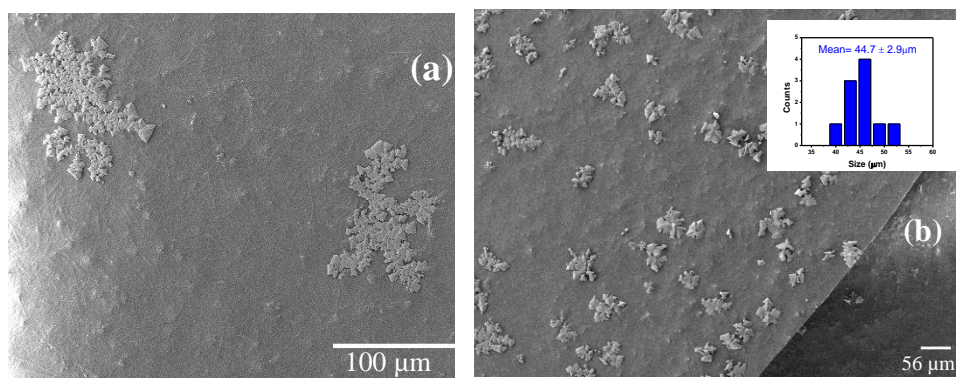


Figure 3.2 E (a) FE- SEM image of PDADMAC. **(b)** FE-SEM image of Ag NPs –polymer mixture.

Due to very small sized Ag NPs, it was difficult to see how they are really attached to polymer after aggregation. So we perform PL microscopy, of

Ag NPs and Ag NPs with 2.5 wt % PDADMAC to see the blinking nature of individual Ag NPs and of aggregated spot with polymer. PL imaging was carried at 477 nm excitation wavelength from an argon ion laser. Figure 3.2 (F) shows the PL imaging of Ag NPs on the glass coverslip. The localized luminescent spots show distinct luminescent blinking (fluorescence on/off) that persists over several minutes.

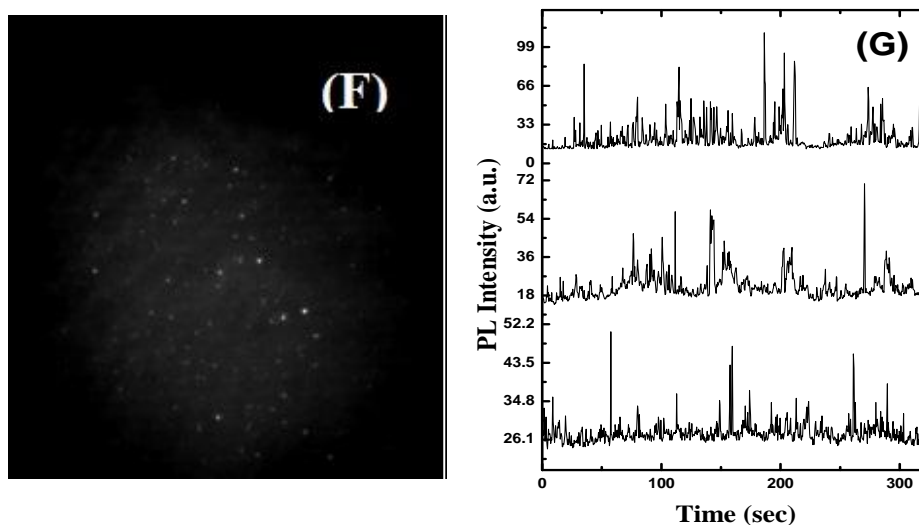


Figure 3.2 (F) PL image of Ag NPs **(G)** PL intensity profile of Ag NPs.

Figure 3.2 (G) shows the time traces of three selected luminescent spots. The random luminescence bursts observed in these time traces indicate the on-events from the citrate-capped Ag NPs. The number of luminescent spots decreases significantly in the presence of 2.5 wt % PDADMAC and shows very few bright and bigger sized luminescent spots. Figure 3.2 (H) shows the PL image of Ag NPs in the presence of 2.5 wt % PDADMAC. These luminescent spots of Ag NPs in the presence of polymer do not show any characteristic luminescent blinking (Figure 3.2 I).

It is well-established that the luminescence of Ag NPs arises due to the formation of emitting Ag NC from silver oxides on the surface of Ag NPs [34-36]. Previously, it has been shown that only those NC that consist of

two to eight Ag atoms can show intense luminescence in the visible region of the electromagnetic spectrum [36]. Hence, the absence of luminescence from Ag NPs solution in the present study indicates the lack of silver oxide formation in solution; however, when these Ag NPs are deposited on the air–glass interface, they exhibit intense luminescence due to the formation of silver oxides on the surface of Ag NPs, which triggers photoactivated emission from Ag NC.

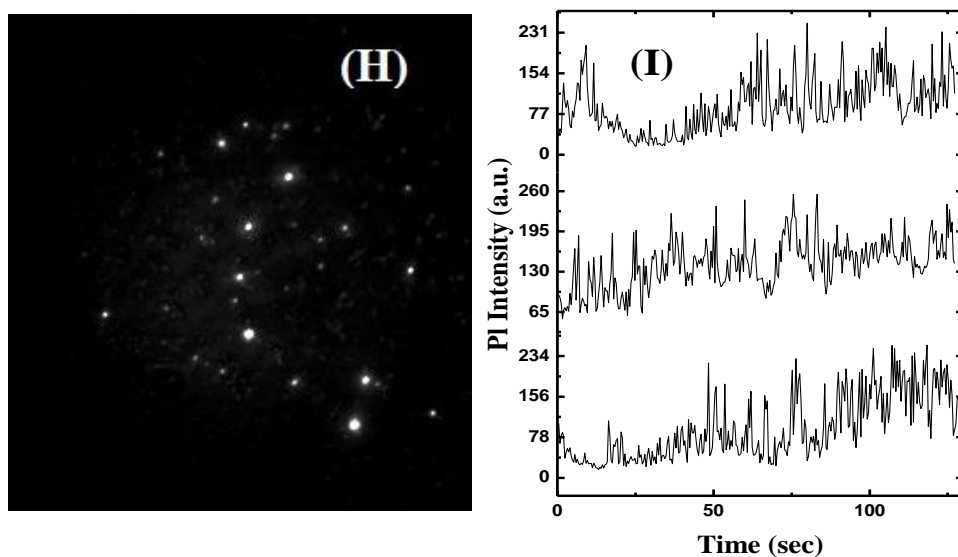


Figure 3.2 (H) PI image (I) PL intensity profile of Ag NPs in the presence of 2.5 wt % PDADMAC.

In addition, the distinct luminescence bursts observed in the time traces of Ag NPs indicate the on-events from these Ag NC; however, diffusion and subsequent aggregation of these Ag NC on the surface of Ag NPs result in the off-events due to the formation of non luminescent NC [37]. On the other hand, the bigger-sized non blinking luminescent spots of Ag NPs in the presence of PDADMAC arise due to the formation of polymer-induced aggregates of Ag NPs. Absence of any distinct photon bursts clearly signifies the lack of silver oxide formation on the Ag NPs surface due to the presence of polymer on top of the citrate-capped Ag NPs.

3.3. Surfactant Induced Aggregation of Ag NPs and its Interaction with PVP

The LSPR band of Ag NPs is centered at 394 nm in the absence of CTAB. The peak position as well as the absorbance of Ag NPs changes progressively upon gradual addition of CTAB up to a concentration of 0.4 mM (Figure 3.3 A). In the presence of 0.2 mM CTAB, Ag NPs show lowest LSPR band centered at 410 nm with a 15 nm red shift. No such spectral changes of Ag NPs have been observed in the presence of negatively charged SDS and neutral TX-100 surfactants (Figure 3.2 C) These spectral changes in the LSPR of Ag NPs in the presence of CTAB indicate the formation of surfactant-induced aggregates of Ag NPs. The observed red shift in the LSPR of Ag NPs is referred to the coupling of the surface plasmon of the closely spaced Ag NPs in the aggregates. Moreover, the absence of any such spectral changes in the presence of negatively charged SDS and neutral TX-100 surfactant indicate that the aggregates are formed due to the specific electrostatic interactions between the negatively charged citrate molecules on the surface of Ag NPs and positively charged CTAB head groups.

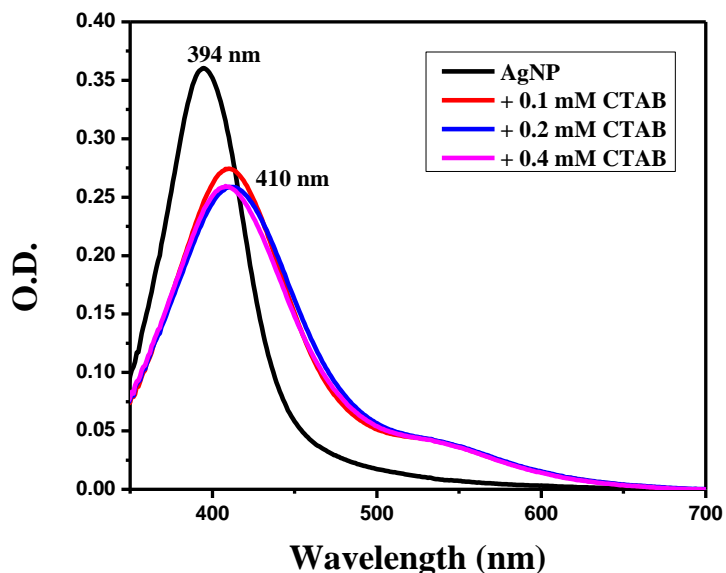


Figure 3.3 A Change in absorption spectra of Ag NPs upon addition of different molar concentration of CTAB

Single-particle PL microscopy experiments have been performed to get the PL characteristics of individual Ag NPs presence of CTAB. Figure 3.3 B shows the PL image of Ag NPs in the presence of 0.2 mM CTAB.

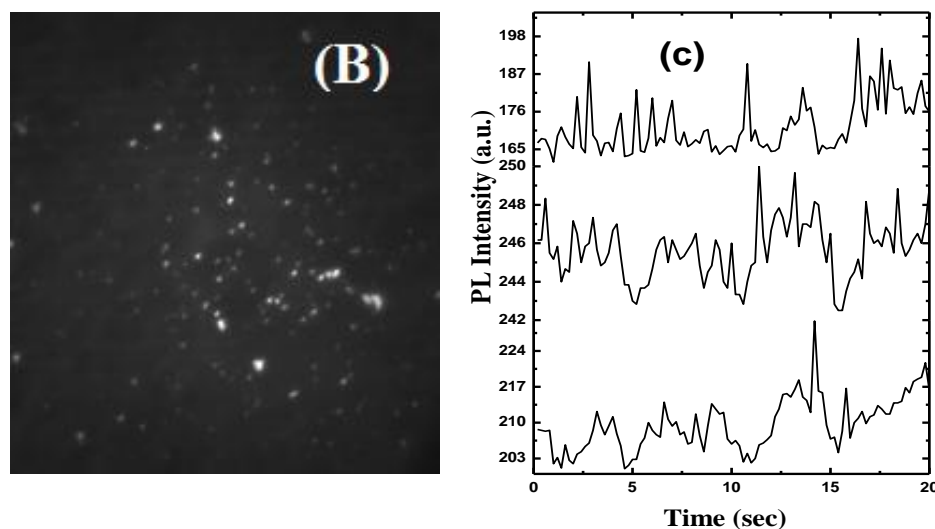


Figure 3.3 (B) PL image **(C)** PL intensity profile of Ag NPs in the presence of 0.2 mM CTAB.

It is evident that in the presence of 0.2 mM CTAB, Ag NPs show very few bright and bigger sized luminescent spots. The natures of the aggregated spots are explained already in section 3.2. After getting aggregated result from CTAB and Ag NPs interaction we further proceed to see how the surfactant is interacting with the polymer PVP. Initially, we carried out absorption spectra of Ag NPs in the presence of 0.2 mM CTAB with 0.5 wt % PVP to see the change in spectra. As expected absorption spectra remains unchanged with suggest that there is no direct interaction between Ag NPs and PVP (Figure 3.3 D). So, to monitor the interaction between surfactant and polymer we perform PL microscopy.

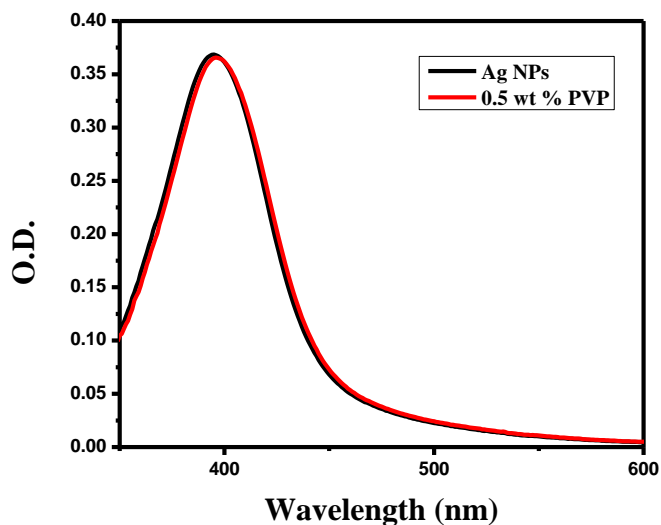


Figure 3.3 D Change in the absorption spectra of Ag NPs in the presence of PVP.

In the presence of PVP some ring type of structures has been observed. As we seen above in the absence of PVP, these CTAB-induced Ag NPs aggregates do not exhibit these kinds of patterns of luminescent spots. Thus, the observed patterns of luminescent spots appear only because of binding of CTAB-induced Ag NPs aggregates with the PVP matrix (Figure 3.3 E and F). Although, it is clear from the absorption spectra of CTAB-induced Ag NPs aggregation remains the same in the absence and presence of 0.5 wt % PVP. Now, there are two possibilities of interaction PVP with the surfactant either hydrophobic chain of surfactant interact with the polymer chain *via* hydrophobic interaction or the positive head group of surfactant interact with the pyrrolidone rings of PVP. From the present concentration of CTAB and PVP it is not clear that what kind of these two interactions are taking place, so we have to choose different concentration of PVP and surfactant to see the proper result of the interaction.

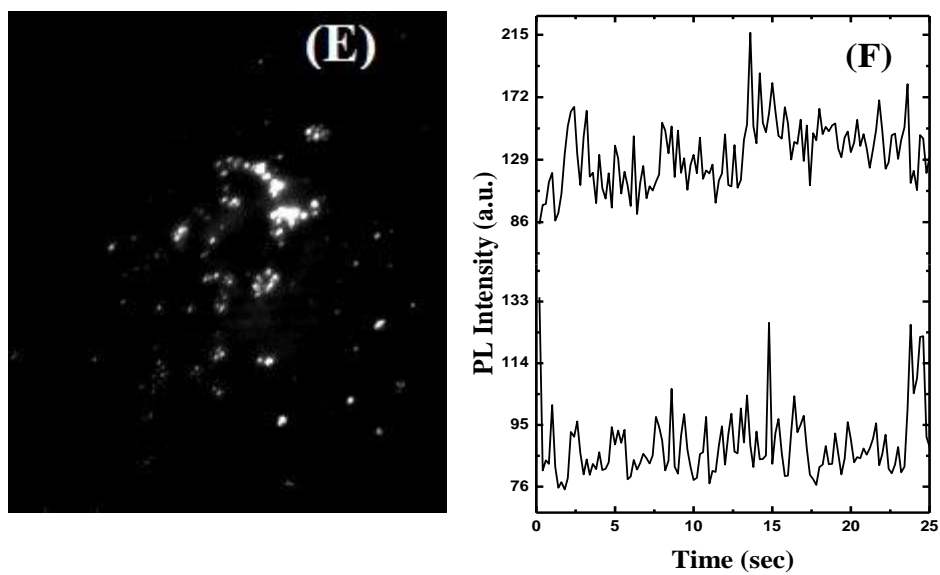


Figure 3.3 (E) PL Image (F) PL intensity profile of CTAB-induced Ag NPs in the presence of 0.5 wt % PVP.

Chapter 4

4. Conclusion and Scope for the Future Work

We have shown the interaction of citrate capped Ag NPs with two different type of polymers and a surfactant which results in aggregation of Ag NPs .In first section we have shown that the negatively charged Ag NPs forms aggregation due to the electrostatic attraction with the positively charged PDADMAC which may be very useful in waste water treatment plants to extract out PDADMAC which is used in purifying the water. On the other hand after confirming the electrostatic interaction taking place between NPs and cationic surfactant CTAB which results in aggregation, we tried to find the interaction taking place between surfactant induced aggregation and neutral polymer. In future, we can try the different concentration of CTAB and PVP to know the proper interaction between them and find out which type of necklace and bead structure will be going to form.

REFERENCES

1. Jin R., Zeng C. and Zhou M., Chen Y. (2016), Atomically precise colloidal metal nanoclusters and nanoparticles: fundamentals and opportunities, *Chem. Rev.*, 116, 10346-10413.
2. Eustis S., El-Sayed M. A. (2006), Why gold nanoparticles are more precious than pretty gold: Noble metal surface plasmon resonance and its enhancement of the radiative and nonradiative properties of nanocrystals of different shapes, *Chem. Soc. Rev.*, 35, 209-217.
3. S. Agnihotri, S. Mukherji and S. Mukherji (2013), Immobilized silver nanoparticles enhance contact killing and show highest efficacy: elucidation of the mechanism of bactericidal action of silver, *Nanoscale*, 5, 7328–7340.
4. Mie, G. Beiträge zur Optik trüber Medien (1908), speziell kolloidaler Metallösungen. *Ann. Phys.*, 330, 377–445.
5. Kreibig U., Vollmer M. (1995), *Optical properties of metal clusters*, Springer, Berlin, Germany (ISBN: 978-3-662-09109-8)
6. S. Agnihotri, S. Mukherji and S. Mukherji (2012), Antimicrobial chitosan–PVA hydrogel as a nanoreactor and immobilizing matrix for silver nanoparticles, *Appl. Nanosci.*, 2, 179–188.
7. Jain P. K., Huang X., El-Sayed I. H., El-Sayed M. A. (2007), Review of some interesting surface plasmon resonance-enhanced properties of noble metal nanoparticles and their applications to biosystems, *Plasmonics*, 2, 107-118.
8. Agnihotri S., Mukherji S., Mukherji S. (2014), Size-controlled silver nanoparticles synthesized over the range 5-100 nm using the same protocol and their antibacterial efficacy, *RSC Adv.*, 4, 3974-3983.
9. Rycenga M., Cobley C. M., Zeng J., Li W., Moran C. H., Zhang Q., Qin D., Xia Y. (2011), Controlling the synthesis and assembly of silver nanostructures for plasmonic applications, *Chem. Rev.*, 111, 3669-3712.

10. Ditlbacher H., Hohenau A., Wagner D., Kreibig U., Rogers, M., Hofer F., Aussenegg F. R., Krenn J. R. (2005), Silver nanowires as surface plasmon resonators, *Phys. Rev. Lett.*, 95, 257403.
11. Nie S., Emory S. R. (1997), Probing single molecules and single nanoparticles by surface-enhanced Raman scattering, *Science*, 275, 1102-1106.
12. Zhang J., Fu Y., Lakowicz J. R. (2007), Enhanced Förster resonance energy transfer (FRET) on a single metal particle, *J. Phys. Chem. C*, 111, 50-56.
13. Gill R., Tian L., Somerville W. R. C., Ru E. C. L., Amerongen H. V., Subramaniam V. (2012), Silver nanoparticle aggregates as highly efficient plasmonic antennas for fluorescence enhancement, *J. Phys. Chem. C*, 116, 16687-16693.
14. Nordlander P., Oubre C., Prodan E., Li K., Stockman M. I. (2004), Plasmon Hybridization in Nanoparticle Dimers, *Nano Lett.*, 4(5), 899–903.
15. Zuloaga J., Prodan E., Nordlander P., Quantum Description of the Plasmon Resonances of a Nanoparticle Dimer (2009), *Nano Lett.*, 9 (2), 887–891.
16. Ghosh S. K., Pal T., Interparticle Coupling Effect on the Surface Plasmon Resonance of Gold Nanoparticles: From Theory to Applications (2007), *Chem. Rev.*, 107 (11), 4797–4862.
17. Lee P. C., Meisel D. (1982), Adsorption and surface-enhanced Raman of dyes on silver and gold sols, *J. Phys. Chem.*, 86, 3391-3395.
18. H. Dautzenberg, W. Jaeger, J. Kotz, B. Philipp, Ch. Seidel, D. Stscherbina(1994), “Polyelectrolytes - Formation, Characterization and Application”, Carl Hanser Publ., Munich, pp 272 (ISBN).
19. F. Caruso, M. Spasova, A. Susha, M. Giersig (2001), R.A. Caruso, Magnetic Nanocomposite Particles and Hollow Spheres Constructed by a Sequential Layering Approach, *Chem. Mater.*, 13, 109–116.

20. Y. Zhu, H. Da, X. Yang, Y. Hu (2003), Preparation and characterization of core-shell monodispersed magnetic silica microspheres, *Colloids Surf. A*, 231, 123–129.
21. Q. Yi, G.B. Sukhorukov (2014), UV-induced disruption of microcapsules with azobenzene groups, *Soft Matter*, 10, 1384–1391.
22. J.E. Wong, W. Richtering (2008), Layer-by-layer assembly on stimuli-responsive microgels, *Curr. Opin. Colloid Interf. Sci.*, 13, 403–412.
23. Ledward, D. A. (1994), In *Protein Functionality in Food Systems*; Hettiarachchy N. S., Ziegler G. R. Eds., Marcel Dekker, New York, p 225.
24. Kendal K., Alford N. McN., Clegg W. J., Birchall J. D. (1989), Flocculation clustering and weakness of ceramics, *Nature*, 339, 130.
25. Wong K., Cabane B., Duplessix R. (1987), Interparticle distances in flocs, *J. Colloid Interface Sci.*, 123, 466–481.
26. Chodanowski P, Stoll S. (2001), Polyelectrolyte adsorption on charged particles in the Debye Hückel approximation, A Monte–Carlo approach, *Macromolecules*, 34, 2320–2328.
27. O. Spalla (2002), Nanoparticle interactions with polymers and polyelectrolytes, *Current Opinion in Colloid & Interface Science* , 7, 179–185.
28. O. Spalla, Cabane B. (1993), Growth of colloidal aggregates through polymer bridging, *Colloid Polym Sci*, 271, 357–371.
29. Trisaranakul W., Chompoosor A., Maneepprakorn W., Nakapricha D., Choengchan N., Teerasong S. (2016), A simple and rapid method based on anti-aggregation of Silver Nanoparticles for the detection of Poly(diallyldimethylammonium chloride) in tap water, *Analytical Science*, 32, 769–773.
30. Prajapati R., Chatterjee S., Bhattacharya A., Mukherjee T. K. (2015), Surfactant-Induced Modulation of Nanometal Surface Energy Transfer from Silicon Quantum Dots to Silver Nanoparticles, *J. Phys. Chem. C*, 119, 13325–13334.

31. Paramelle D., Sadovoy A., Gorelik S., Free P., Hobley J., Fernig D. G. (2014), A rapid method to estimate the concentration of citrate capped silver nanoparticles from UV-Visible light spectra, *Analyst*, 139, 4855-4861.
32. Tuinier R., Rieger J., de Kruif C. G. (2003), Depletion-Induced Phase Separation in Colloid-Polymer Mixtures, *Adv. Colloid Interface Sci.*, 103 (1), 1–31.
33. Ye X., Narayanan T., Tong P., Huang J. S., Lin M. Y., Carvalho B. L., Fetters L. J. (1996), Depletion Interactions in Colloid-Polymer Mixtures, *Phys. Rev. E: Stat. Phys., Plasmas, Fluids, Relat. Interdiscip. Top.*, 54 (6), 6500–6510.
34. Peyser L. A., Vinson A. E., Bartko A. P., Dickson R. M. (2001), Photoactivated Fluorescence from Individual Silver Nanoclusters. *Science*, 291, 103–106.
35. Zheng J., Dickson R. M. (2002), Individual Water-Soluble Dendrimer-Encapsulated Silver Nanodot Fluorescence, *J. Am. Chem. Soc.*, 124, 13982–13983.
36. Geddes C. D., Parfenov A., Gryczynski I., Lakowicz J. R. (2003), Luminescent Blinking from Silver Nanostructures, *J. Phys. Chem. B*, 107, 9989–9993.
37. Wu X., Yeow E. K. L. (2008), Fluorescence Blinking Dynamics of Silver Nanoparticle and Silver Nanorod Films, *Nanotechnology*, 19, 035706.